This is a repository copy of *NO2 hotspots: are we measuring in the right places?*.

Article:

NO₂ hotspots: Are we measuring in the right places?

Michael Beckwith[a], Elizabeth Bates[b], Andrew Gillah[b], Nicola Carslaw[a],*

[a] *Environment Department, University of York, York, YO10 5DD, UK*
[b] *City of York Council, West Offices, Station Rise, York, YO1 6GA, UK*

HIGHLIGHTS

- Road-side monitoring of nitrogen dioxide concentrations at a variety of intersections.
- Assessment of road intersection traffic behaviour, environmental variables and impact on nitrogen dioxide concentrations.
- Comparison of nitrogen dioxide concentrations at road junctions against in-situ monitors.

ARTICLE INFO

ABSTRACT

Nitrogen Dioxide (NO₂) is a major atmospheric pollutant which is produced from a variety of anthropogenic sources, notably vehicular emissions. High NO₂ concentrations are found in and around the urban environment and as such pose a significant threat to human health. Diffusion tube surveys of NO₂ concentrations were carried out at a variety of intersections and road layouts over a 3-month period in 2017. This study identified that 'hotspots' in NO₂ concentrations frequently occurred in sections of road where vehicles are accelerating or queueing. Under these conditions, concentrations were elevated by 58.6% and 52.6% respectively compared to when vehicles were cruising. Analysis of environmental factors which influence NO₂ concentrations show that meteorology, topography, traffic volume and driver behaviour all contribute. The results highlight the complexity of monitoring hotspot locations and show the need for traffic and driver behaviour to be included in vehicle emission models. Additionally, the investigation suggests need for caution when relying on in-situ monitors to determine pollutant exceedances as there is shown to be substantial variation along a street and the location of the monitor is critical.

1. Introduction

Nitrogen dioxide (NO₂) is a major airborne pollutant which contributes to a variety of adverse health effects. (WHO, 2005; COMEAP, 2015). For instance, a recent report from the UK Committee on the Medical Effects of Air Pollutants (COMEAP, 2015) considered current evidence to conclude that short and long-term exposures to NO₂ are likely to have impacts on human morbidity and mortality rates. Strak et al. (2013) suggest that short term exposure to NO₂ likely increases thrombin production and hence results in an elevated risk of stroke, myocardial ischaemia and coronary heart disease. In addition, there are increases in asthma incidence resulting from exposures to NO₂ (EPA, 2015). Short and long-term exposure of children to NO₂, at all stages of development, show this group has specific susceptibility. Effects include neo-natal weight reduction, when mothers experience third trimester exposure (Huang et al., 2015), and asthma morbidity amongst pre-

school children (Hansel et al., 2008). Furthermore, NO₂ exposure has been linked to asthma exacerbations amongst primary school-aged children (YoussefAgha et al., 2012) and reduced lung function for paediatrics (Trasande and Thurston, 2005). Finally, long term exposure to NO₂ has been linked to higher incidence of lung disease (Soto-Martinez and Sly, 2010).

Nitrogen oxides (NO$_X$ = Nitric oxide (NO) + NO₂) are emitted from motor vehicles in large quantities in urban areas. Consequently, a key exposure pathway to NO₂ for humans is time spent in urban environments, especially when in proximity to vehicles, either as pedestrians or as passengers (Molle et al., 2013). Pedestrian routes through cities are often adjacent to roads and high pedestrian volume routinely coincides with periods of high traffic volume, such as commuting to work and school. This can result in people receiving short term exposures to concentrations of pollutants, which could potentially exceed recommended limits. The recognised adverse health effects of NO₂
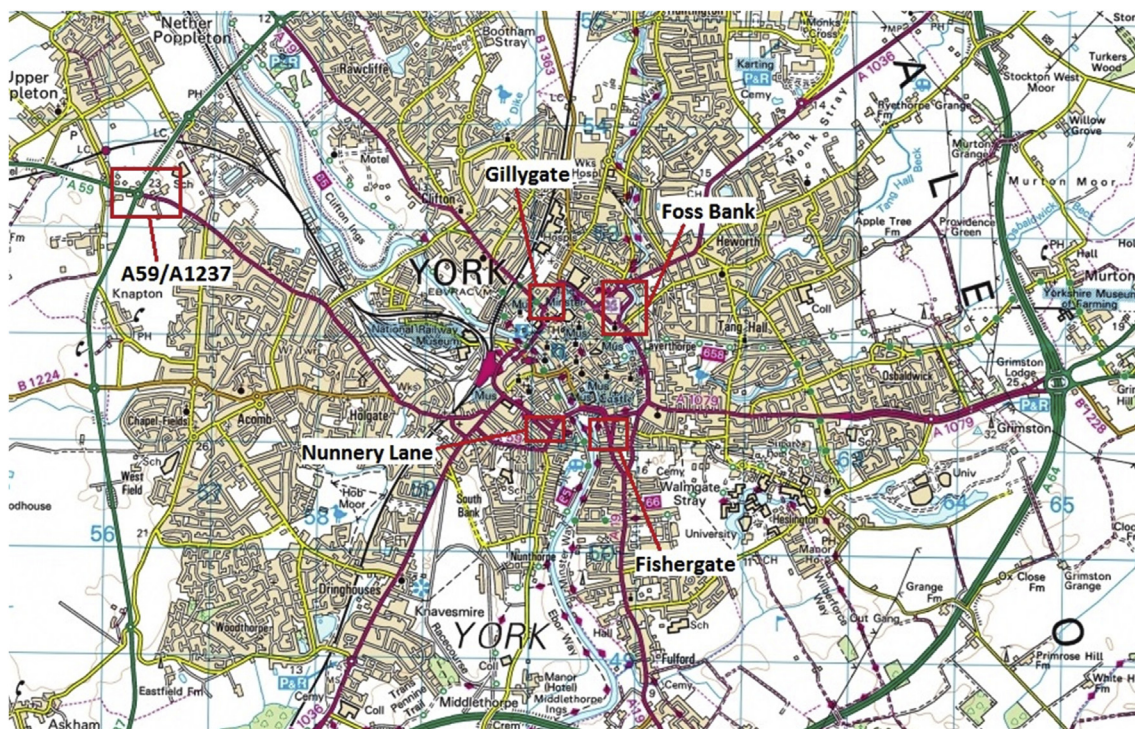

Fig. 1. Overview of the study sites across the City of York (Bing maps, 2017). The five study sites (red boxed areas) are labelled. (For interpretation of the references to colour in this figure legend, the reader is referred to the Web version of this article.)

exposure has resulted in the European Council issuing two limit values: an annual mean value of $40 \, \mu gm^{-3}$ and an hourly value of $200 \, \mu gm^{-3}$ with 18 exceedances of the latter permitted per year (Council Directive, 1999/30/EC). It should be noted, however, that the health benefits of exercise (e.g. walking, cycling), potentially outweigh the effects of exposure to pollutants on busy streets (Tainio et al., 2016).

The climate change agenda has necessitated a reduction in CO_2 emissions, resulting in the UK government until recently, incentivising road-users to use diesel-powered vehicles as a more fuel-economical alternative to petrol vehicles. The proportion of diesels vehicles in the total fleet is now higher compared to times before the incentive was introduced (Department for Transport, 2016a,b) although recent decreases in sales figures for diesels have been reported in response to proposed surcharges (Society of Motor Manufacturers and Traders, 2018). The competition in the vehicle sales sector has led to the recent dieselgate scandal, whereby a manufacturer has resorted to misleading emission tests in order to continue to show improved performance in millions of diesel cars (Brand, 2016). Diesel vehicles use higher engine temperatures than petrol vehicles, which result in higher concentrations of NOx as a fraction of the total exhaust gas emissions (AQEG, 2004; Lozhkina and Lozhkin, 2016). In recent years, developments in exhaust gas control systems such as diesel oxidation catalysis, exhaust gas recirculation, lean NOx trap and selective catalytic reduction have been designed to reduce NOx levels to meet increasingly stringent Euro emission targets set by the EU and the UK (Resitgolu et al., 2015). Whilst these measures have reduced overall levels of NOx, the fraction of NO_2 has increased (Grice et al., 2009). Consequently, NO_2 exceedances are still frequently observed in many urban environments when a decline might have been expected (Carslaw et al., 2011).

The behaviour of drivers in the urban environment has been studied at length with the emissions of vehicles depending heavily on road layout, traffic conditions, car type, engine type and installed vehicle technology (Pandian et al., 2009). Queuing traffic during congested periods means idling engines which has been associated with elevated NO_2 emissions as a function of distance travelled (O'Driscoll et al., 2016). New technologies are increasingly being developed with the aim

of reducing both fuel consumption and air pollution whilst engines are idling in queuing traffic (Yang et al., 2014). However, the phasing-in of such technologies is protracted and many older vehicles are still present on the roads. On a local scale authorities and communities have campaigned and in some cases legislated against idling, with resulting evidence showing some positive impacts with respect to air quality (Ryan et al., 2013).

The apparent benefits aside, such anti-idling campaigns may have taken focus away from emissions at junctions potentially leading the public to think that idling traffic is the main contributor to local ambient air pollution problems. However, exhaust emission research (Frey et al., 2003) has shown that spikes in emission gases occur where vehicles are accelerating away from junctions and engines are consequently under greater load.

This study aims to measure NO_2 concentrations ($[NO_2]$) at several locations along road junctions in an urban environment, to identify potential hotspots where the measured concentration exceeds $40 \, \mu gm^{-3}$. By comparing our results with those from nearby regulatory in-situ monitors, we can ascertain the representativeness of such site locations for quantifying local air pollutant concentrations. The study also aims to determine the environmental drivers of the $[NO_2]$ at each site by investigating local meteorology, traffic counts, topographic data (distance from kerb and degree of urban canyon) and traffic regime data.

2. Methods

2.1. Study area

The measurements were carried out in the city of York, which has a population of $\approx 200,000$ (City of York Council, 2011) and ≈ 7 million tourist visitors annually (Visit York, 2015). Many city centre streets are relatively narrow, flanked by 3–5 storey buildings. Vehicular access to the largely pedestrianised city centre is limited, which results in large vehicle numbers on the encircling roads (Fig. 1). Traffic flow on these roads is controlled by a variety of interchanges and one-way systems,

despite which, there is frequently congestion at peak times of the day. Encompassing the larger suburban area of York is a ring road which, to the west and north of the city is a single carriageway punctuated by roundabouts, routinely congested at peak times. The topography in this area has an open aspect, as it generally passes through flat agricultural land.

As a result of exceedances of set Limit Values (Council Directive, 1999/30/EC), the city centre roads fall within an imposed Air Quality Management Area (AQMA), the consequences of which are Air Quality Action Plans (AQAP) which detail numerous measures to reduce emission-based pollutants (City of York Council, 2017). The monitoring of pollutant concentrations is carried out by seven automatic air samplers, one of which is linked to the national DEFRA Automatic Urban and Rural Network (AURN). The monitors are located at sites adjacent to busy junctions, predominantly on the busy roads which circle the historic city centre.

2.2. Diffusion tubes

A modified DEFRA (2008) protocol was employed for preparation and analysis of NO_2 diffusion tubes. To prepare the diffusion tubes, gauzes were first rinsed with acetone and drained over a beaker, then soaked in triethanolamine/acetone solution (200 ml of acetone mixed with 224.4 g of triethanolamine) for 30 min. After draining, two gauzes were placed into the grey end cap of a diffusion tube, which was then capped at the other end with a cream end cap. The prepared tubes were kept refrigerated in sealed plastic bags until use. The tubes were exposed in triplicate for a period of 12–14 days at a time. They were positioned 2.2 m above the ground and on street furniture wherever possible, away from vertical surfaces in accordance with DEFRA (2008) recommendations. Travel blanks, laboratory blanks and rural background controls were analysed in the same way as the samples.

Standards were prepared using a 150 mg/l sodium nitrite solution ($\equiv$ 100 ppm NO_2). to make a range of standard solutions for calibration equivalent to 0, 0.5, 1.0, 1.5, 2.0 ppm (example calibration curve is provided in Supplementary information S1). A sulphanilamide/phosphoric acid reagent was prepared by adding 25 ml orthophosphoric acid to ~300 ml of deionised water, followed by 10 g of sulphanilamide. The mixture was stirred and made up to 500 ml with deionised water. NEDD (N-(1-Naphthyl)ethylenediamine dihydrochloride) reagent was made by dissolving 1.4 g of NEDD in 250 ml of deionised water.

To analyse the tubes, the cream caps were removed and 1.5 ml of deionised water was added to each and left for 20 min. At that stage, 1.5 ml of sulphanilamide/phosphoric acid reagent was added to each tube followed by 0.15 ml of NEDD reagent. The tubes were recapped, agitated and left for 30 min. The absorbance of the resulting solution (for samples, laboratory, travel blanks and rural exposure controls) in each tube was then measured at 520 nm using a spectrophotometer and the NO_2 concentration calculated using the calibration curve and the protocol defined by DEFRA (2008) (S2). The resultant concentrations were scaled to incorporate the bias adjustment factor (0.78) derived by Air Quality England (2015) to standardise diffusion tube measurements with in-situ monitors.

To improve precision in the measurements, means of the triplicate data from each sampling point were calculated and outliers were omitted if they were outside 20% of mean values, in-line with guidance from DEFRA (2008). In addition, a 14 day co-location study, using the nearest available City of York Council in-situ NO_2 monitors, was executed to validate the diffusion tube data. Triplicate diffusion tubes were positioned directly adjacent to three monitors located at Gillygate, Nunnery Lane and Heworth Green near to northern end of Foss Bank (Figs. 1 and 2 c, d, e).

2.3. Pilot study

A pilot study was carried out at a variety of road locations to identify potential study sites. The ring road (A1237/A59) roundabout is a major intersection on the outskirts of the city with several points of queuing and accelerating traffic. The Fishergate one-way system is a complex junction with traffic congestion during peak times. Foss Bank is a section of urban one-way road where traffic is consistently accelerating, then cruising/slowing, then queuing. Gillygate is a traffic-light controlled intersection in a congested, narrow (width $\approx$ 12 m) street canyon, where traffic is predominantly queuing and accelerating. Nunnery Lane is a one-way system where traffic is predominantly slowing/queuing and accelerating in adjacent sections. At these sites, triplicate diffusion tubes were exposed for 12 days.

It was determined from the pilot study that all sites showed a variation in [NO_2] depending on position along the intersection. Extra sampling points at the ring road (A59/A1237) roundabout were included for the full study (points E − J) to provide data on the approach to and departure from the roundabout along the A59. The addition of the qualitative traffic regime categories (accelerating, cruising and queuing) for the sites can be seen in Fig. 2.

2.4. Auxiliary data

The Urban Terrain Zones (UTZ) classification (low, medium, high) (Grimmond and Oke, 1999) describes the dimensions and layout of buildings and other obstacles which might contribute to the formation of street canyons, with subsequent wind flows resulting in eddies that impact on [NO_2] at the different study sites. A qualitative classification of the study sites was carried out using the UTZ as a reference. In addition, the aspect ratio (AR) of the street cross section (Height/Width) was used as a metric for the size of the urban canyon. Furthermore, the horizontal distance from the sampling point to the kerb was measured to account for any changes in concentrations as distances from the emission sources varied.

Meteorological data (atmospheric pressure, temperature, windspeed and direction) were downloaded from the Linton-on-Ouse weather station (latitude = 54.047, longitude = −1.2515) for each sampling period (Meteoblue, 2017). Precipitation (rainfall) data was downloaded from the University of York, Department of Electronics Data Archive (2017) and the daily data was averaged over each exposure period (S4). When the site displayed urban canyon qualities the AR was used to differentiate between a skimming flow regime (AR $\geq$ 0.5) and a wake interface flow/isolated roughness flow (AR < 0.5) (Vardoulakis et al., 2003). When AR < 0.5 the wind speed and direction were assumed to be unaffected by the buildings present. When the AR $\geq$ 0.5, i.e.: a street canyon, any winds which were perpendicular (angle of incidence = 90° ± 15°) to the street were assumed to be skimming over the top of the canyon. Such winds were not included in the analysis presented in section 3.2, as the magnitude of the wind speed affecting the dispersion of [NO_2] at street level would be different from that recorded at the weather station (Savory et al., 2004). Wind parameters were represented as windroses generated in the Openair package (Carslaw, 2015).

A qualitative assessment of the typical traffic behaviour at each location was carried out at peak flow times, using on-site observations and the typical traffic flow representation (Googlemaps, 2017). The predominant status of the traffic at each location during peak flow periods was noted and these were categorised into either: accelerating, cruising or queuing (a combination of idling and accelerating).

Traffic flow data were taken from the Department for Transport database (DfT, 2016a,b) using the average annual daily flow estimates from 2016 (S10). The data were grouped into four categories depending on vehicle type: cars/motorcycles; buses/coaches; light goods; heavy goods. For the Fishergate, Nunnery Lane and Foss Bank sites, the traffic count data were considered indicative of the traffic flow. There were no traffic data for Gillygate, hence, the mean traffic data from adjacent roads which feed into Gillygate were calculated (from Museum Street, Bootham, Lord Mayor's Walk). Similarly, the mean traffic counts which
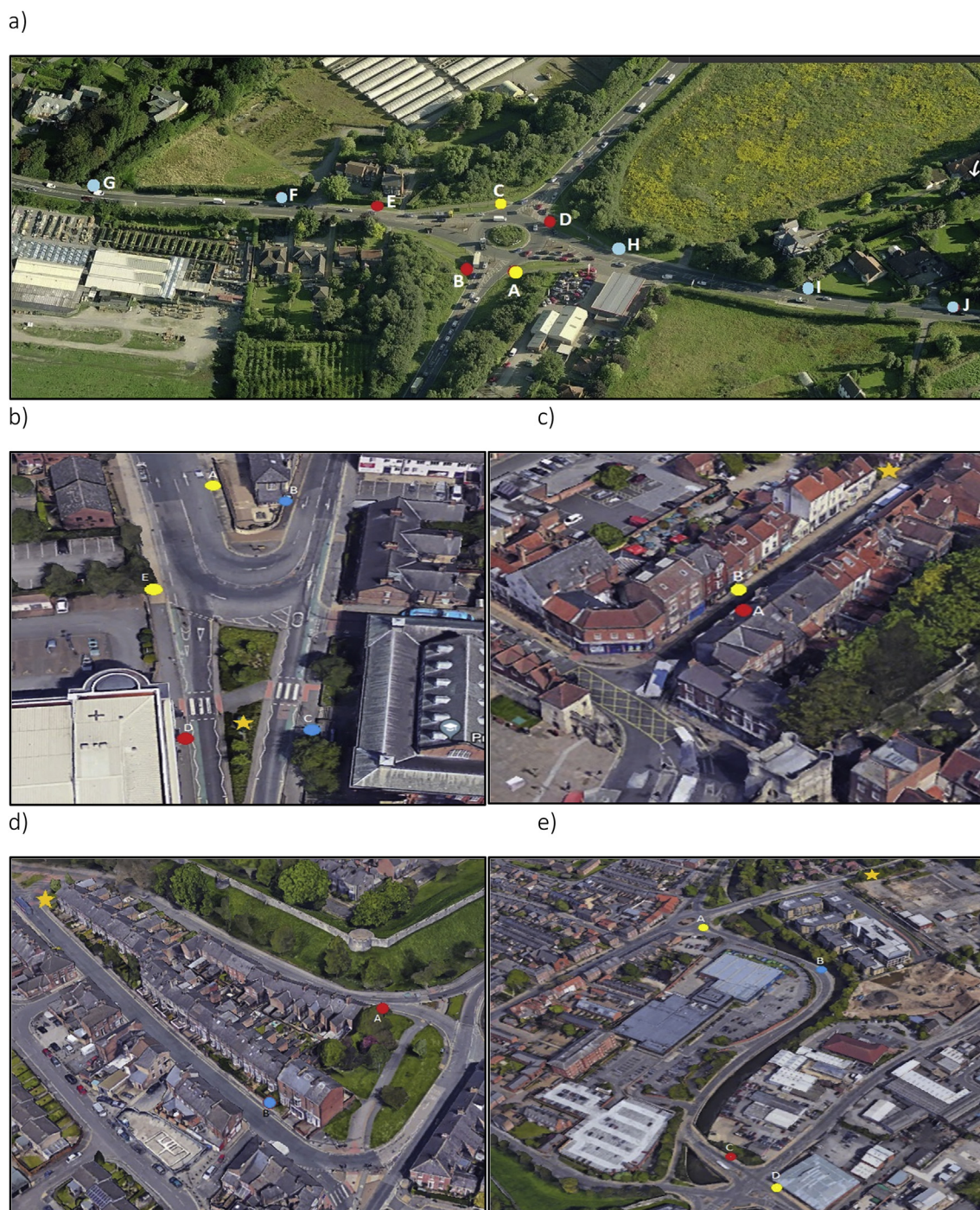
a)

b) c)

d) e)

Fig. 2. Aerial photographs from due South (Microsoft, 2017) of a) Ring road (A59/A1237) roundabout, b) Fishergate one-way system, c) Gillygate/Bootham junction, d) Nunnery Lane/Prices Lane one-way system and e) Foss Bank. Labelled points (A–J) of the diffusion tubes at each location where traffic predominantly accelerates (yellow), queues (red) and cruises/slows (blue) during peak traffic times. In-situ monitor locations (yellow star). (For interpretation of the references to colour in this figure legend, the reader is referred to the Web version of this article.)

feed into the A59/A1237 roundabout (Fig. 2a, locations A, B, C, D) were calculated and for the locations solely on the A59 (Fig. 2a, locations E − J) a mean of the traffic count data from west and east side of the roundabout was used respectively. These daily flow estimates were then scaled up to the full exposure period (12–14 days). The absence of any dedicated traffic data for the specific study sites and period meant that the traffic counts were only used qualitatively in the analysis in section 3.3. Normalisation of values was carried out using the z-score method.

Statistical analysis and figures were generated using R (R Core Team, 2017). Welch t-tests were carried out to determine the presence of any significant differences in the [NO_2] between sampling points at each site. The p values were subjected to a multiple testing adjustment using the false discovery rate (FDR) post-hoc test (Benjamini and Hochberg, 1995). Kruskal-Wallis rank sum test (with pairwise Wilcoxon rank sum test) was employed to reveal any significant differences in [NO_2] between the traffic regimes.

To determine which environmental variables contribute to the [NO_2] at each site, the predictor variables: traffic counts (petrol, diesel bus, diesel light goods and diesel heavy goods); meteorological data

(wind speed, wind direction, atmospheric pressure, air temperature, precipitation); urban canyon AR metric; distance to kerb; traffic regime, were analysed in the R environment. Note that once data associated with specific wind directions were removed as explained in the Methods, the remaining winds were turned into vectors in the form, ws*cos(θ). Then, at sites where the aspect ratio was ≥0.5 these vectors were used in the analysis as a predictor variable. Gaussian variables were transformed to fulfill the requirements of the statistical tests (Zuur et al., 2010). Following the removal of any intercorrelated transformed predictor variables (variable inflation factors < 5) (Zuur et al., 2010) the remaining variables to be modelled were checked for pairwise intercorrelation using Pearson Coefficients (r ≤ 0.7) (Dormann et al., 2012). Models were generated in a Gaussian regression linear model (LM) followed by a stepwise backward-forward selection, using Akaike Information Criterion (AIC). Starting with a full model, this technique was employed to remove variables which did not contribute to the response variable significantly. The produced minimum adequate models for each site were subsequently checked against their respective full model to determine change in deviance using an analysis of deviance F test.

3. Results

3.1. Quality control and co-location with in situ monitors

Laboratory blanks, travel blanks and rural background [NO$_2$] were measured for each of the 5 exposure periods (Fig. 3). The rural background measurements were made in a rural location which was > 50 m from a minor road. (longitude = −0.7079, latitude = 53.9229). The travel and laboratory blanks confirmed that there was no significant contamination of the tubes with the mean concentration for each run < 1 μgm^{-3}. These background tubes showed the diffusion tubes were measuring background [NO$_2$] in the same range as DEFRA (2017) monitors, i.e. 1–3 μgm^{-3}.

Table 1 shows the results of a 14-day colocation study between triplicate sets of diffusion tubes and in-situ monitors at three of the study sites. Student's *t-tests* were carried out to determine the presence of any significant differences in the [NO$_2$] recorded by diffusion tubes and [NO$_2$] recorded by the CYC in-situ monitor. This analysis showed no significant (95% level) differences between the two methods at all three sites.
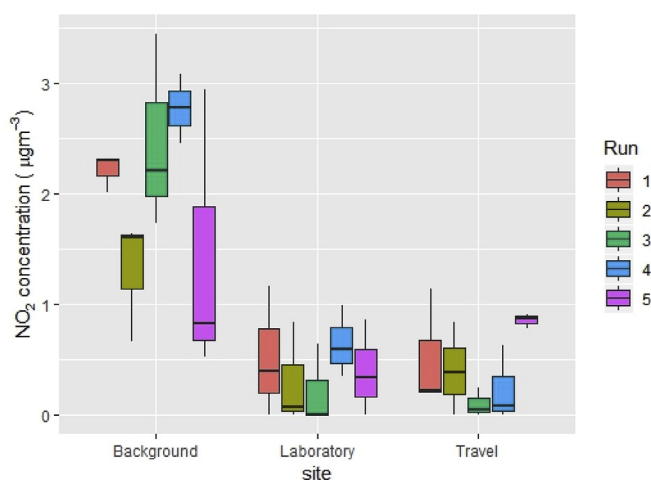

Fig. 3. [NO$_2$] (μgm^{-3}) from the rural background site, laboratory blanks, and travel blanks; (n = 3). Box plots show inter quartile range (IQR), with whiskers indicating 1.5*IQR.

Table 1
Co-location validation of the diffusion tubes. Comparison of the mean concentration from triplicate diffusion tubes at each site with the mean concentration from hourly CYC monitor data over the same exposure period. Included statistics: mean (x̄), standard deviation (σ), sample size (n), *t-test* p-value (p$_t$). Note the high σ values for the monitor data show the variability of [NO$_2$] over the exposure periods.

Location	[NO$_2$] (μgm^{-3}) Diff Tubes			[NO$_2$] (μgm^{-3}) Monitor			p$_t$
	x̄	σ	n	x̄	σ	n	
Nunnery Lane	17.90	0.89	3	16.17	9.23	234	0.051
Heworth Green (Foss Bank)	16.36	1.30	3	15.77	5.67	346	0.063
Gillygate	17.85	1.63	3	19.40	10.78	343	0.236

3.2. NO$_2$ concentration intra-site comparisons

The cumulative values from the A59/A1237 site (Fig. 4a) along with the *t-test* adjusted p-values (S3) suggest that the ambient [NO$_2$] are in the sequence C > A = B > D > E = F = G = H = I = J. Points C and A had accelerating traffic, B and D queuing and the other points predominantly cruising vehicles. Differences between accelerating points A and C may be caused by higher engine loads at point C as drivers increase acceleration anticipating an uphill gradient to the north. Traffic at point A is accelerating away from the intersection but on to a road with no gradient, hence, lower engine loads.

There is a gradual reduction in measured [NO$_2$] as distance from the roundabout increases, except for point F, which shows a higher mean value when compared to adjacent sample points, possibly due to its proximity to a bus stop (Fig. 4a). The westerly A59 approach (points E and F) to the roundabout when compared to the easterly exit (points I and J) show higher [NO$_2$], possibly attributable to traffic queuing at E and F but cruising at I and J.

Generally, Fig. 4 shows that there is some temporal variation between the sites for different sampling periods. These relate to the differences in traffic volume between term time (Pilot, run 2 and 3) and school holidays (run 4 and 5), and to differences in wind speeds and directions and other pollutant concentrations (e.g. ozone, see S9) over the entire sampling period.

[NO$_2$] from the Fishergate site (Fig. 4b) and the *t-test* adjusted p-values (S3) show that the ambient [NO$_2$] follow the sequence A = E = B = D > C. A and E had accelerating traffic, D queuing vehicles and point C cruising vehicles. There is more uncertainty at the Fishergate site compared to the others, caused by missing data at point D and a loss in precision at point B for run 4. The proximity of B to A could explain non-significant differences in the recorded concentration and why point B had higher than expected [NO$_2$]. A and B record similar [NO$_2$] except during run 3 and 5 when site B was higher, possibly due to stronger south westerly winds during these periods (Fig. 5c, e).

The traffic regime categories at the Foss Bank site were accelerating traffic at A and D, queuing vehicles at C and point B having vehicles which were cruising or decelerating. The ambient [NO$_2$] (Fig. 4d) are in the sequence A = C = D > B. The Foss Bank site displayed [NO$_2$] which approached the limit level at locations A, C and D, and these were marginally higher (p$_t$ = 0.047) than the nearest CYC in-situ monitor on Heworth Green.

The cumulative [NO$_2$] from the Gillygate site (Fig. 4c) and the *t-test* adjusted p-values (S3) suggest that the ambient [NO$_2$] are in the sequence A < B. The significantly lower [NO$_2$] (p < 0.025) between run 5 and the other exposure periods correspond to a high proportion of winds blowing near parallel to the orientation of the street canyon, perhaps leading to increased dispersion of the pollutant (Fig. 5e). The mean [NO$_2$] during runs 2–4, show a much smaller difference between A and B, when a significant proportion of wind flowed perpendicular to
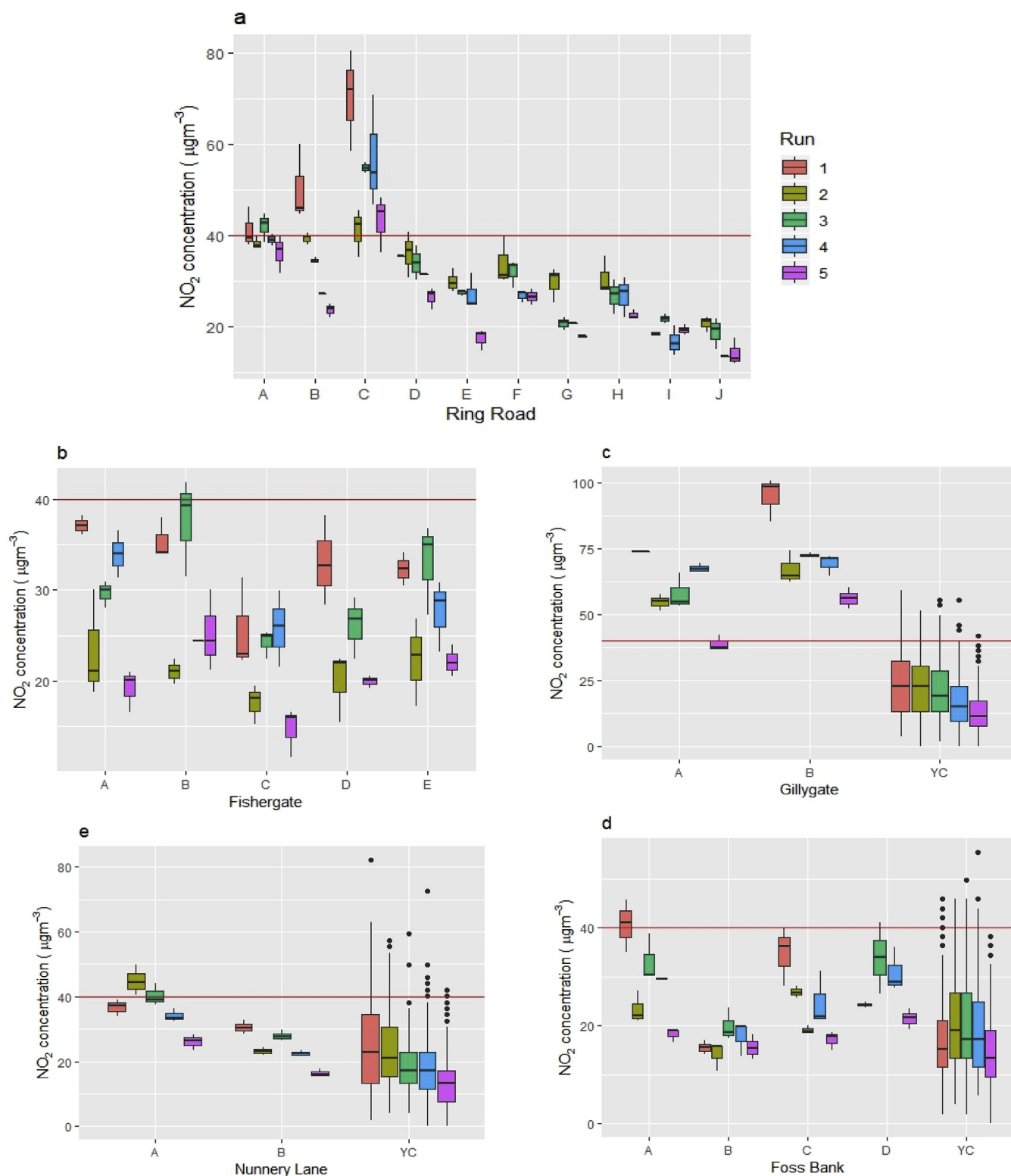
Fig. 4. [NO$_2$] (µgm^{-3}) at each sampling point for a) Ring road, b) Fishergate, c) Gillygate, d) Foss Bank, and e) Nunnery lane, Box plots show inter quartile range (IQR), with whiskers indicating 1.5*IQR and outliers (black dots). For comparison, CYC is hourly [NO$_2$] taken from City of York in-situ monitor data. Locations shown in Fig. 2. Red line indicates EU annual mean limit value. (For interpretation of the references to colour in this figure legend, the reader is referred to the Web version of this article.)

Gillygate (north westerlies or south easterlies) (Fig. 5b, c, d), leading to skimming flow across the top of the canyon as observed in this street previously by Boddy et al. (2005) for carbon monoxide. In the majority of exposure periods Gillygate exceeded the [NO$_2$] limit value and was

significantly higher ($p_t = 0.001$) than the CYC monitor situated ≈ 30 m along the street (Fig. 4c).

The cumulative [NO$_2$] from the Nunnery lane site (Fig. 4e) and the *t*-test adjusted p-values (S3) suggest that the ambient [NO$_2$] are in the
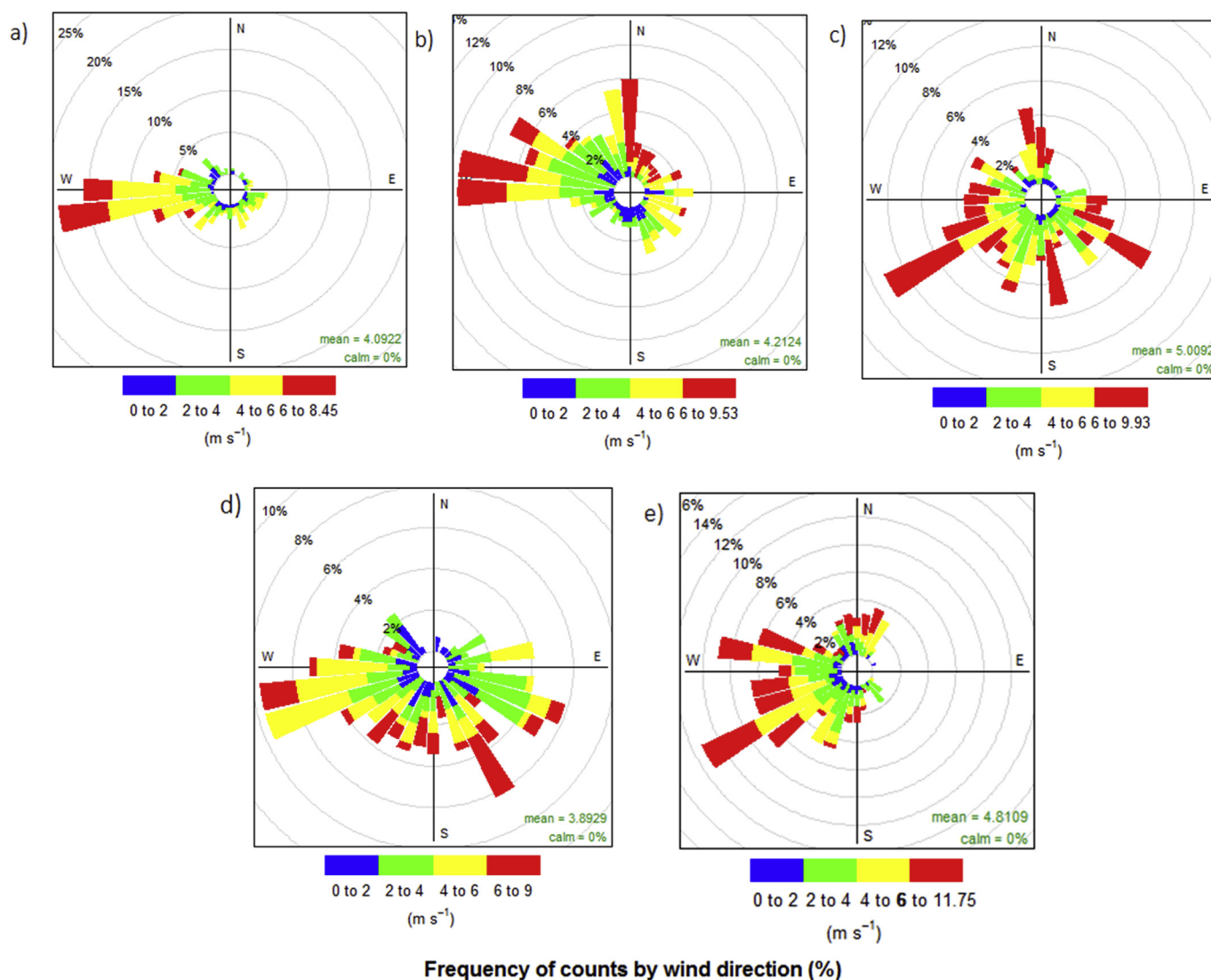
Fig. 5. Wind roses showing the wind speed (ms^{-1}) and direction for the exposure periods: a) Pilot (25/5/17–6/6/17); b) Run 2 (14/6/17–26/6/17); c) Run 3 (26/6/17–7/7/17); d) Run 4 (17/7/17–31/7/17); e) Run 5 (31/7/17–14/8/17).

sequence A > B. There is a significant difference between the sampling points for each run, but Nunnery Lane displays the opposite trend as the other sites with regards to the traffic regime; slowing and queuing traffic at A is consistently associated with higher [NO$_2$] when compared to the accelerating regime at B. The CYC monitor located ≈100 m to the north west of the study area recorded significantly lower [NO$_2$] (p_t > 0.001) than at the selected sampling points, which further exemplifies the large variation in concentrations along the urban street.

3.3. Effects of environmental variables on [NO$_2$]

Analysis of the whole data set in relation to the traffic regime shows [NO$_2$] increasing as the engine load of the vehicles increases from cruising to queuing and accelerating (Fig. 6). A Kruskal-Wallis test shows a significant difference in the mean [NO$_2$] for the traffic regimes (p < 0.001, χ^2 = 57.86). Pairwise comparisons using a Wilcoxon rank sum test revealed that there was a significant difference between cruising and both the queuing and accelerating regimes (p < 0.001).

There was an expected positive correlation between traffic count data and [NO$_2$] (S11). Analysis of the ratio of diesel to petrol vehicles showed a positive correlation between [NO$_2$] and the number of diesel vehicles as a proportion of the total fleet. Dissecting the diesel portion of the fleet into LGV, Bus and HGV revealed that both LGVs and HGVs

are positively correlated to [NO$_2$]. When [NO$_2$] is normalised against traffic count data, a positive correlation with the canyon aspect ratio is revealed, with [NO$_2$] increasing as the canyon becomes more pronounced. Also, there is a negative (albeit small) correlation between the distance of the sample point from the kerb and [NO$_2$] (S12).

Hourly meteorological data was averaged for each exposure period. A small positive correlation was found between [NO$_2$] and ambient air temperature (S5); whilst total precipitation (S7) and atmospheric pressure (S6) showed a negligible negative relationship with [NO$_2$]. Analysis of wind speeds suggested a negative correlation (S8) with [NO$_2$] as concentrations were diluted by dispersion during higher average wind speeds.

Linear Models (LM) for each of the sites were produced incorporating the environmental variables. Once intercorrelated variables had been removed, the AIC selection was performed on the data from the different sites to produce a minimum adequate model (MAM) (Table 2). In each case predictor variables which influenced the [NO$_2$] for that specific site are shown.

The number of vehicles was the main driver for [NO$_2$]. . Except for Fishergate and Gillygate, traffic regime had an influence on [NO$_2$], with the A59/A1237 roundabout and Foss Bank displaying higher concentrations where traffic was predominantly accelerating, though the opposite trend was seen at Nunnery Lane. For Fishergate, the lower %
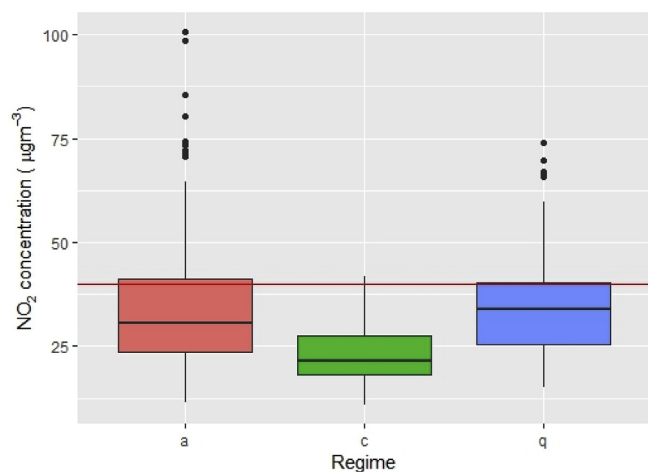
Fig. 6. [NO$_2$] from all sites categorised into locations where traffic was accelerating (a) (n = 129), cruising (c) (n = 88) and queuing (q) (n = 79). The box plots show inter quartile range (IQR), with whiskers indicating 1.5*IQR and outliers (black dots). Red line indicates EU annual mean limit value. (For interpretation of the references to colour in this figure legend, the reader is referred to the Web version of this article.)

Table 2
Full models and minimum adequate models (MAM) produced by Akaike Information Criterion (AIC) for each of the sampled sites with test statistics: % of deviance (%D) explained. *P* values to show analysis of deviance (F test) between MAMs and their respective full models. Sample size (n). Slope coefficients of individual predictor variables. For explanations of variable abbreviations see Methods 2.4.

Variable Set	AIC	%D	*P* (F test)	N	slope
Ringroad: Full	807.9	72.0		110	
MAM: log$_n$ car	807.9	72.0	–	110	+18.16
canyon					−34.59
air temperature					+1.501
regime					
Fishergate: Full	407.1	59.1		60	
MAM: kerb	403.9	58.6	0.71	62	−3.494
log$_n$ bus					−4.193
canyon					−25.93
atmos pressure					−1.128
Gillygate: Full	186.7	86.4		23	
MAM: log$_n$ bus	186.7	86.4	–	23	−84.77
atmos pressure					−1.087
regime					–
wind					+7.182
Nunnery Lane: Full	175.34	73.4		23	
MAM: log$_n$ bus	174.89	71.9	0.264	24	−44.07
regime					–
atmos pressure					−0.050
Foss Bank: Full	341.38	63.5		47	
MAM: kerb	341.23	62.2	0.206	48	−0.5961
log$_n$ bus					−39.54
wind speed					−5.446
regime.					–

Deviance exemplifies the complexities of pollution dispersion in the urban environment and suggest the presence of factors influencing [NO$_2$] not measured in this study. In more detail, the absence of influence of the traffic regime at this site could be attributed to the higher than expected [NO$_2$] at point B. Generally, each site displayed different environmental drivers with traffic flow counts, wind velocity and topographic variables shown to influence the [NO$_2$] to different degrees.

4. Discussion

There were found to be significant differences in the [NO$_2$] within

the studied sites between areas with accelerating, queueing or cruising traffic. The observation at several of our studied sites that [NO$_2$] increased when engines were under load support the study by Kean et al. (2003), who also found higher pollutant concentrations in an uphill tunnel when there was increased loading on vehicle engines. Unal et al. (2004) determined that significant predictor variables for pollutant concentrations were the speed and acceleration metrics of seven different models of car. In addition, Cédric et al. (2016) showed that hotter diesel engines (during acceleration) emit 10–300% more NO$_2$, depending on the after-treatment systems installed. Where the link between acceleration and high [NO$_2$] was not observed in this study, it appears that other drivers such as wind velocity, canyon effect, and traffic numbers were important.

When considering points A – D at the A59/A1237 site, there was a significant difference between the sites when engines were under load compared to those where they were not. Points C and A stand out as locations where [NO$_2$] frequently exceed the EU limit value (> 40 µgm^{-3}) (Fig. 4a). Analysis from Foss Bank also showed higher [NO$_2$] at points A, C and D compared to B where vehicles are cruising, although this may be the result of dispersed NO$_2$ from nearby large intersections which have larger traffic flows. Similarly, the significantly lower [NO$_2$] at points which were solely on the A59 (E -J) as opposed to those on the roundabout (A – D) would almost certainly be influenced by the lower traffic flows. Chaney et al. (2011) produced a decay curve for NO$_2$ heading perpendicularly away from a major road. The decrease (≈50%) in [NO$_2$] from point D to point J on the A59 (150 m) is notably larger than the decrease measured by Chaney et al. over a similar distance (≈300 m).

The variability of [NO$_2$] around the study sites highlighted the limitations in reliance on single in-situ monitors on a road as, in several cases, these were not representative of the [NO$_2$] at nearby sampling points. A large discrepancy between sampling points and the adjacent monitor was seen at the Gillygate site with a 3-fold difference in [NO$_2$] recorded over a 30 m stretch of road. The use of in-situ monitoring data will be indicative of local [NO$_2$] but will not preclude the existence of nearby hotspots which exceed the limit value.

In addition to the effects of traffic regime and vehicle counts, NO$_2$ hotspots can be related to a specific source. In this study, the bus stop at point F (Fig. 4a) might explain the elevated concentrations when compared to adjacent points along the intersection. A similar, but less significant difference can be seen at the Fishergate site where point E (also a bus stop) has higher measured concentrations than adjacent point C (Fig. 4b). The high-resolution mapping carried out by Apte et al. (2017) provides further evidence of highly localised sources of NO$_2$.

Results highlighted that the combined effects of meteorological and topographical variability on [NO$_2$] could conceal traffic related variables. The one-way system and adjoining roads at the Fishergate site produced results showing significantly higher [NO$_2$] at B than A, which went against the observed traffic regime (Fig. 4b). The Fishergate site was shown to be predominately influenced by the canyon effect, wind speed and the distance to kerb variables (Table 2). In this study the distance from the sampling tube to the exhaust outlet of vehicles was simplified to the distance to the kerb. This simplification may not have given a true representation of this actual distance, due to carriageway size and the position of vehicles on the road. Closer scrutiny of traffic behaviour at the U-bend adjacent to A at Fishergate revealed that vehicles are further from the kerb than at the other sample points potentially resulting in lower [NO$_2$].

In addition to the meteorological data, driver behaviour and kerb distance variables, analysis suggests the Fishergate site [NO$_2$] are influenced by the variations in street canyon aspect ratios at the different sampling points. Samples taken at the northern end of the site, where the aspect ratios are lower, show higher [NO$_2$]. Possible reasons for this could be that southerly/westerly winds, which predominated during the data collection period, acted to disperse the pollutants away from the sample points at the southern end of Fishergate and towards the

other sampling points. However, the complexity of the junction, including the various side streets, asymmetrical canyons and obstacles, makes any inferences regarding the site's topographic effect on $[NO_2]$ very speculative, given the spatial resolution of this study.

Analysis showed other impacts on $[NO_2]$ which could not definitely be attributed to the traffic regime. At the Gillygate site for two of the five periods there were temporary traffic lights at the north east end of Gillygate where it meets Lord Mayor's Walk (Fig. 2c), leading to queuing traffic on both sides of the road. The proximity of the two sample points may have been such that there was negligible difference between the distance from the exhaust pipes of the vehicles from either lane to the diffusion tubes. Further, the canyon effect of Gillygate (AR = 1.1) could have led to mixing of the pollutants at lower heights concealing any differences resulting from the observed traffic regimes. Indeed, as highlighted in Boddy et al. (2005), air flows from adjoining roads (Bootham, St. Leonard's Place and Portland Street) may have had a significant influence on the wind flow patterns on Gillygate and hence, the dispersion of $[NO_2]$ in the different exposure periods.

The complexity of urban roughness and air turbulence on the $[NO_2]$ is further exemplified at the Nunnery Lane site. It displays the opposite trend when compared to the other sites with point A (queuing traffic) having higher concentrations than at point B (accelerating traffic). Point A has cruising/slowing traffic which forms queues at peak times due to congestion formed by two pedestrian crossings and traffic lights over the Skeldergate Bridge. The two roads which make up the two lengths of the Nunnery Lane one-way system are both orientated to roughly the same degree (A ≈ 135°, B ≈ 140°) and as such should experience a similar degree of dispersion from the background winds. Reasons for the larger concentrations at A could be simply a result of increased traffic numbers, although the estimated DfT data suggests equivalent numbers on both sections of road. An alternative reason could be due to the sampling points experiencing a canyoning effect when the background wind blows from either a westerly or south westerly direction. At point A (Fig. 3e) a bank of tall trees to the North of the road could deflect south westerly winds down. This would establish a primary canyon vortex that would reverse the wind direction at road level and move the vehicle emissions, concentrating them towards point A. The opposite would occur at B with the primary vortex moving pollutants from the vehicle exhaust to the opposite side of the road, not towards point B. A more detailed assessment of the wind movements would have to be undertaken to confirm this hypothesis.

5. Conclusions

This investigation has shown the existence of NO_2 hotspots within intersections which are influenced by traffic behaviour. When a comparison was made with the regulatory in-situ monitors, two of the three additional sites had markedly higher $[NO_2]$. All sites, most notably the ring road (A1237/A59) roundabout and Gillygate, exceeded the EU limit value. There is a positive correlation between $[NO_2]$ and road sections where vehicle engines are frequently under increased load. Diesel vehicles were likely to have contributed more to measured roadside $[NO_2]$, although the exact category of vehicles passing the sample points could not be determined from the study. The results from this research, particularly the presence of hotspots, could have implications regarding compliance of local authority AQMAs to NO_2 limits. An in-situ monitor will give an indication of local air quality but is unlikely to identify all locations along an intersection where air quality limits are exceeded. The results also suggest that a traffic behaviour metric should be included in dispersion models at the local/street scale.

Acknowledgements

Appendix A. Supplementary data

Supplementary data to this article can be found online at https://doi.org/10.1016/j.aeaoa.2019.100025.

References

Air Quality England, 2015. Local Diffusion Tube Bias Adjustment Spreadsheet (XLS). Air Quality England, UK. Available at: http://www.airqualityengland.co.uk/laqm , Accessed date: 15 July 2017.

Air Quality Expert Group, 2004. Nitrogen Dioxide in the United Kingdom. Defra Publications, London.

Apte, J.S., Messier, K.P., Gani, S., Brauer, M., Kirchstetter, T.W., Lunden, M.M., Marshall, J.D., Portier, C.J., Vermeulen, R.C.H., Hamburg, S.P., 2017. High-resolution air pollution mapping with google street view cars: exploiting big data. Environ. Sci. Technol. 51 (12), 6999–7008.

Benjamini, Y., Hochberg, Y., 1995. Controlling the false discovery rate: a practical and powerful approach to multiple testing. J. R. Stat. Soc. Ser. B 57 (1), 289–300.

Boddy, J.W.D., Smalley, R.J., Dixon, N.S., Tate, J.E., Tomlin, A.S., 2005. The spatial variability in concentrations of a traffic-related pollutant in two street canyons in York, UK— Part I: the influence of background winds. Atmos. Environ. 39, 3147–3161.

Brand, C., 2016. Beyond 'Dieselgate': implications of unaccounted and future air pollutant emissions and energy use for cars in the United Kingdom. Energy Policy 97, 1–12.

Carslaw, D.C., 2015. Openair: Open-Source Tools for Analysing Air Pollution Data. King's College London, UK Available at: http://www.openair-project.org/Default.aspx, Accessed date: 1 July 2017.

Carslaw, D.C., Beevers, S.D., Tate, J.E., Westmoreland, E.J., Williams, M.L., 2011. Recent evidence concerning higher NOx emissions from passenger cars and light duty vehicles. Atmos. Environ. 45, 7053–7063.

Cédric, L., Goriaux, M., Tassel, P., Perret, P., André, M., Liu, Y., 2016. Impact of after-treatment device and driving conditions on black carbon, ultrafine particle and NOx emissions for Euro 5 diesel and gasoline vehicles. Transportation Research Procedia 14, 3079–3088.

Chaney, A.M., Cryer, D.J., Nicholl, E.J., Seakins, P.W., 2011. NO and NO₂ interconversion downwind of two different line sources in suburban environments. Atmos. Environ. 45, 5863–5871.

City of York Council, 2011. Headline Figures for York (Census 2011). City of York Council, UK. Available at: https://www.york.gov.uk/info/20037/statistics_and_information/79/census , Accessed date: 21 July 2017.

City of York Council, 2017. AQMAs in York. City of York Council, UK Available at: http://jorair.co.uk/air-quality-in-york/aqmas, Accessed date: 12 August 2017.

Committee on the Medical Effects of Air Pollutants, 2015. Statement on the Evidence for the Effect of Nitrogen Dioxide on Health. COMEAP, Public Health England Available at: https://www.gov.uk/government/uploads/system/uploads/attachment_data/file/411756/COMEAP_The_evidence_for_the_effects_of_nitrogen_dioxide.pdf, Accessed date: 7 July 2017.

European Communities (1999) 1999/30/EC, D. Council Directive, 1999. 30/EC of, 22 April, 1999. Relating to limit values for sulphur dioxide, nitrogen dioxide and oxides of nitrogen, particulate matter and lead in ambient air (The First Daughter Directive). Official Journal of the European Communities L163/41.

Department for Environment Food & Rural Affairs, 2008. Diffusion Tubes for Ambient NO₂ Monitoring: Practical Guidance for Laboratories and Users. DEFRA, London. Available at: https://laqm.defra.gov.uk/documents/0802141004_NO2_WG_PracticalGuidance_Issue1a.pdf , Accessed date: 6 June 2017.

Department for Transport, 2016a. Traffic Count Datasets. Department for Transport, UK Available at: https://www.dft.gov.uk/traffic-counts/cp.php?la = York, Accessed date: 7 July 2017.

Department for Transport, 2016b. Vehicle Licensing Statistics: Annual 2016. Department for Transport, UK. Available at: https://www.gov.uk/government/uploads/system/uploads/attachment_data/file/608374/vehicle-licensing-statistics-2016.pdf , Accessed date: 12 December 2017.

Dormann, C., Elith, J., Bacher, S., Buchmann, C., Carl, G., Carré, G., Marquéz, J., Gruber, B., 2012. Collinearity: a review of methods to deal with it and a simulation study evaluating their performance. Ecography 36 (1), 27–46.

EPA, 2015. Integrated Science Assessment for Oxides of Nitrogen – Health Criteria (Second External Review Draft). United States Environmental Protection Agency. Available at: http://cfpub.epa.gov/ncea/isa/recordisplay.cfm?deid = 288043 , Accessed date: 7 July 2015.

Frey, H.C., Unal, A., Rouphail, N.M., Colyar, J.D., 2003. On-road measurement of vehicle Tailpipe emissions using a portable instrument. J. Air Waste Manag. Assoc. 53 (8), 992–1002.

Googlemaps, 2017. Maps of York, UK. Google, USA. Available at: https://www.google.co.uk/maps/@53.9586771,-1.1506319,12z , Accessed date: 20 June 2017.

Grice, S., Stedman, J., Kent, A., Hobson, M., Norris, J., Abbott, J., Cooke, S., 2009. Recent trends and projections of primary NO₂ emissions in Europe. Atmos. Environ. 43, 2154–2167.

Grimmond, C.S.B., Oke, T.R., 1998. Aerodynamic properties of urban areas derived from analysis of surface form. J. Appl. Meteorol. 38 (9), 1262–1292.

Hansel, N.N., Breysse, P.N., McCormack, M.C., Matsui, E.C., Curtin-Brosnan, J., Williams,

D.L., Moore, J.L., Cuhran, J.L., Diette, G.B., 2008. A longitudinal study of indoor nitrogen dioxide levels and respiratory symptoms in inner-city children with asthma. Environ. Health Perspect. 116 (10), 1428–1432.

Huang, C., Nichols, C., Liu, Y., Zhang, Y., Liu, X., Gao, S., Li, Z., Ren, A., 2015. Ambient air pollution and adverse birth outcomes: a natural experiment study. Popul. Health Metrics 13, 17.

Kean, A.J., Harley, R.A., Kendall, G.,R., 2003. Effects of vehicle speed and engine load on motor vehicle emissions. Environ. Sci. Technol. 37 (17), 3739–3746.

Lozhkina, O.V., Lozhkin, V.N., 2016. Estimation of nitrogen oxides emissions from petrol and diesel passenger cars by means of on-board monitoring: effect of vehicle speed, vehicle technology, engine type on emission rates. *Transport. Res.,* Part D 47, 251–264.

Meteoblue, 2017. Weather History Download RAF Linton-on Ouse. Meteoblue, Basel, Switzerland Available at: https://www.meteoblue.com/en/weather/archive/export/raf-linton-on-ouse_united-kingdom_6296673, Accessed date: 1 August 2017.

Microsoft, 2017. Bing Maps. Microsoft Corporation, Redmond, Washington Available at: https://www.bing.com/maps, Accessed date: 3 July 2017.

Molle, R., Mazoué, S., Géhin, E., Ionescu, A., 2013. Indoor/outdoor relationships of airborne particles and nitrogen dioxide inside Parisian buses. Atmos. Environ. 69, 240–248.

O'Driscoll, R., ApSimon, H.M., Oxley, T., Molden, N., Stettler, M.E.J., Thiyagarajah, A., 2016. A Portable Emissions Measurement System (PEMS) study of NOx and primary NO_2 emissions from Euro 6 diesel passenger cars and comparison with COPERT emission factors. Atmos. Environ. 145, 81–91.

Pandian, S., Gokhale, S., Ghoshal, A.-K., 2009. Evaluating effects of traffic and vehicle characteristics on vehicular emissions near traffic intersections. *Transport. Res.* Part D 14, 180–196.

R Core Team, 2017. R: A Language and Environment for Statistical Computing. R Foundation for Statistical Computing, Vienne, Austria Available at: http://www.R-project.org/, Accessed date: 2 February 2017.

Resitoglu, I.A., Altinisik, K., Keskin, A., 2015. The pollutant emissions from diesel-engine vehicles and exhaust after treatment systems. Clean Technol. Environ. Policy 17, 15–27.

Ryan, P.H., Reponen, T., Simmons, M., Yermakov, M., Sharkey, K., Garland-Porter, D., Eghbalnia, C., Grinshpun, S.A., 2013. The impact of an anti-idling campaign on outdoor air quality at four urban schools. Environ. Sci.: Processes and Impacts 15, 2030.

Savory, E., Rotach, M.W., Chauvet, C., Guilleteaou, E., Kastner-Klein, P., KovarPanskus, A., Louka, P., Sahm, P., Trini Castelli, S., 2004. Street architecture and air quality. In: Berkowicz, R., Britter, R., Di Sabatino, S. (Eds.), Optimisation of Modelling Methods for Traffic Pollution in Streets TRAPOS.

Society of Motor Manufacturers and Traders, 2018. SMMT New Car Registrations. SMMT, London, UK. Available at: https://www.smmt.co.uk/vehicle-data/car-registrations/ , Accessed date: 28 February 2018.

Soto-Martinez, M., Sly, P.D., 2010. Relationship between environmental exposures in children and adult lung disease: the case for outdoor exposures. Chronic Respir. Dis. 7 (3), 173–186.

Strak, M., Hoek, G., Steenhof, M., Kilinc, E., Godri, K.J., Gosens, I., Mudway, I.S., van Oerle, R., Spronk, H.M.H., Cassee, F.R., Kelly, F.J., Harrison, R.M., Brunekreef, B., Lebret, E., Janssen, N.A.H., 2013. Components of ambient air pollution affect thrombin generation in healthy humans: the RAPTES project. Occup. Environ. Med. 70 (5), 332.

Tainio, M., de Nazelle, A.J., Götschi, T., Kahlmeier, S., Rojas-Rueda, D., Nieuwenhuijsen, M.J., de Sá, T.H., Kelly, P., Woodcock, J., 2016. Can air pollution negate the health benefits of cycling and walking? Prev. Med. 87, 233–236.

Trasande, L., Thurston, G.D., 2005. The role of air pollution in asthma and other paediatric morbidities. J. Allergy Clin. Immunol. 155 (4), 689–699.

Unal, A., Frey, H.C., Roupail, N.M., 2004. Quantification of highway vehicle emissions hot spots based upon on-board measurements. J. Air Waste Manag. Assoc. 54 (2), 130–140.

University of York, Department of Electronics, 2017. Data Archive. University of York, UK. Available at: https://weather.elec.york.ac.uk/archive.html , Accessed date: 29 June 2017.

Vardoulakis, S., Fisher, B.E.A., Pericleous, K., Gonzalez-Flesca, N., 2003. Modelling air quality in street canyons: a review. Atmos. Environ. 37 (2), 155–182.

Visit York, 2015. Research and Statistics. Make it York, UK. Available at: http://www.visityork.org/members/about/statistics.aspx , Accessed date: 21 July 2017.

World Health Organisation, 2005. Air Quality Guidelines for Particulate Matter, Ozone, Nitrogen Dioxide and Sulfur Dioxide Global Update 2005 Summary of Risk Assessment. World Health Organisation, Switzerland Available at: http://apps.who.int/iris/bitstream/10665/69477/1/WHO_SDE_PHE_ OEH_06.02_eng.pdf, Accessed date: 15 March 2017.

Yang, K.-C., Kuo, C.-T., Chen, C.-Y., Yang, C.-C., Wu, C.-M., Huang, C.-M., 2014. Frequency-based vehicle idling detection. International Journal of Automation and Smart Technology 4 (1).

YoussefAgha, A.H., Jayawardene, W.P., Lohrmann, D.K., El Afandi, G.S., 2012. Air pollution indicators predict outbreaks of asthma exacerbations among elementary school children: integration of daily environmental and school health surveillance systems in Pennsylvania. J. Environ. Monit. 14, 3202.

Zuur, A., Ieno, E., Elphick, C., 2010. A protocol for data exploration to avoid common statistical problems. Methods in Ecology and Evolution 1 (1), 3–14.